

Content from this work may be used under the terms of the CC BY 3.0 licence (© 2018). Any distribution of this work must maintain attribution to the author(s), title of the work, publisher, and DOI.

# FABRICATION AND TEST OF $\beta=0.3$ 325MHz BALLOON SINGLE SPOKE RESONATOR\*

Z. Yao<sup>†</sup>, J. Keir, D. Kishi, D. Lang, R. E. Laxdal, H. Liu, Y. Ma, B. Matheson, B. S. Waraich, Q. Zheng, V. Zvyagintsev, TRIUMF, Vancouver, Canada

## Abstract

A novel balloon variant of the single spoke resonator (SSR) has been designed, fabricated and tested at TRIUMF. The cavity is the  $\beta=0.3$  325 MHz SSR1 prototype for the Rare Isotope Science Project (RISP) in Korea. The balloon variant is specifically designed to reduce the likelihood of multipacting barriers near the operating point. A systematic multipacting study led to a novel geometry, a spherical cavity with re-entrant irises plus a spoke. The balloon cavity provides competitive RF parameters and a robust mechanical structure. Cold tests demonstrated the principle of the balloon concept. The fabrication experience and the preliminary test results will be reported in this paper.

## INTRODUCTION

RISP has been proposed as a multi-purpose accelerator facility at the Institute for Basic Science (IBS), Korea, for research in atomic and nuclear physics, material science, bio and medical science, etc. At the heart of RISP is a powerful heavy ion linac. [1] The linac consists of three independently phased superconducting sections. The high energy section SCL2 of the driver linac uses two types of 325 MHz single spoke resonators with geometry  $\beta$  at 0.30 and 0.51 corresponding to SSR1 and SSR2 respectively. TRIUMF has been contracted to design, fabricate and test two of the SSR1 variants

The prototype cavity of SSR1  $\beta=0.30$  designed by TRIUMF is shown in Figure 1. The cavity is termed the balloon variant due to the conformal shape of the outer conductor that obviates the need for a central spool. The balloon geometry is proposed to suppress multipacting in the accelerating gradient range of several MV/m [2]. It also provides a more inherently robust mechanical structure. The cavity is designed [3] to operate in continuous wave (CW) mode at 2 K with 35 MV/m peak electric field. The design parameters are listed in Table 1.



Figure 1: SSR1 prototype cavity.

Table 1: Design Parameters of SSR1.

Parameters	Value
Frequency	325 MHz
Geometry $\beta$	0.30
Geometry factor	93 $\Omega$
R/Q	233 $\Omega$
$E_{peak}/E_{acc}$	3.84
$B_{peak}/E_{acc}$	6.07 mT/(MV/m)
df/dp	-1.6 / +1.5 Hz/mbar
Lorentz force detuning	-8.7 / -1.4 Hz/(MV/m) <sup>2</sup>
Tuning sensitivity	467 kHz/mm

## CAVITY FABRICATION

The SSR1 prototype is fabricated with 3 mm RRR niobium for cavity, and 3 mm 316L stainless steel for the helium jacket. The bare cavity consists of two half shells, one spoke, plus beam and RF ports, shown in Figure 2.

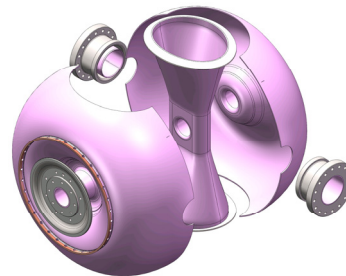


Figure 2: Explosion view of SSR1.

The spoke is deep drawn and EB welded. Two collars are added as transitions between spoke and cavity shells. As a sequence, access is available to the RF surface of the most critical welds at the roots of spoke. They are at the peak magnetic field region, and require full penetration welds with smooth inner surface finish. The balloon geometry also requires a minimal fillet radius at these joints to obtain the optimal suppression effect of the first order multipacting barrier. The position and thickness fits between collar and shells are critical to the final welding, and require special care during fabrication.

Spinning is chosen to form the half shells. Comparing to deep drawing, it is a cost-efficient technique for prototype with over 500mm diameter. The shell is spun in two steps. The nose cone at the centre area is spun with the roller on the RF surface with the die on the opposite side. The peripheral area is done in the reverse way with a second die. A disadvantage of spinning is the difficulty in achieving a constant wall thickness. A variable shell thickness can af-

\* Work supported by RISP – TRIUMF Collaboration

<sup>†</sup> zyyao@triumf.ca

fect cavity mechanical properties, such as the pressure sensitivity. The shell thickness varies from 1.5 mm to 3.0 mm along the cavity radial profile and varies slightly from shell to shell. The thinnest area is about 100 mm away from equator, where the large stretching occurs in spinning. For this reason deep drawing of half shells is recommended for cavity mass production due to the more consist forming.

The cavity beam nose with beam tube is machined from bulk niobium. The material thickness is increased at the beam nose to eliminate the requirement of additional ribs. The thickened material also provide opportunity to adjust cavity frequency by trimming the nose during fabrication.  $\pm 2$  mm trimming allowance is left on each nose, which promises  $\pm 1.9$  MHz frequency adjustment range. The RF stack-up measurement is done with complete half shells and spoke without collars. The cavity frequency is then adjusted by trimming the nose cones, and followed by the equator weld and the collar welds.

The flanges are 316L stainless steel prepared for Helicalflex Seal. Vacuum brazing is applied to the connections to niobium. Tungsten inert gas (TIG) welding is also used between copper and niobium for the stiffening ring which is attached to helium jacket.

## CAVITY PROCESSING

The first prototype cavity was inspected and leak checked after fabrication. 200  $\mu\text{m}$  surface layer was removed by buffer chemical polishing (BCP) in several steps with flipping cavity orientation. The BCP solution is mixed with  $\text{HNO}_3$ , HF,  $\text{H}_3\text{PO}_4$  in the volume ratio of 1:1:2. The cavity is fixed on a support frame via stiffener rings on both end shells, shown in Figure 3. The RF ports are positioned up and down during etching. RF ports are used as acid inlet and outlet. The acid temperature was monitored during etching and controlled below 15  $^\circ\text{C}$ . A niobium coupon is utilized at the outflow port to estimate the etching rate and the etching amount. The differential etching was observed by measuring cavity resonant frequency in between each step. Due to the significant contrast of the cavity volume and the diameter of acid flow ports, acid has obvious velocity change. In addition, the spoke and nose cones on shells sit on the pathway of acid flow. It enhances turbulence and the differential etching effect.

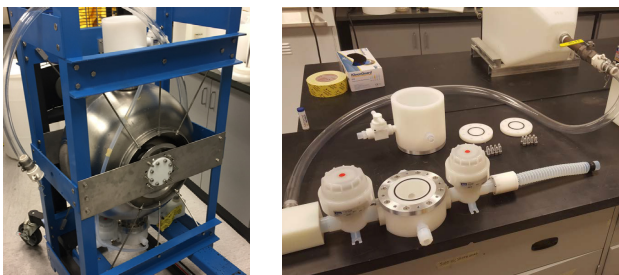


Figure 3: Cavity frame and etching fixtures.

High pressure rinsing (HPR) is done through beam ports on the horizontal rinsing stand and each RF port on the vertical rinsing stand, shown in Figure 4. A dedicated nozzle is designed for this cavity. There are two water jets on each

direction from 30  $^\circ$  to 150  $^\circ$  off the rinsing wand axis with an increment of 30  $^\circ$ . Two additional water jets are 10  $^\circ$  off the axis on the top. For each cavity assembly, the cavity was rinsed 3.5 hours on the horizontal stand at 80bar pressure, and 2 hours on vertical stand via each RF port with 45bar pressure.



Figure 4: Horizontal HPR (left) and vertical HPR (right).

The cavity was degassed after an integrated 200 $\mu\text{m}$  BCP. There were obvious signs of hydrogen Q-disease in the pre-degassing tests. Due to concerns about the copper brazing between niobium and stainless-steel flanges, 600 $^\circ\text{C}$  for 10 hours degassing recipe was selected. The hydrogen partial pressure was monitored with residual gas analyser (RGA), and reduced by 3 orders of magnitude. Additional 20  $\mu\text{m}$  BCP followed by HPR was completed prior to cold test.

Low temperature baking was applied as the last treatment for the hermetic seal cavity before cold test. Two recipes, 50  $^\circ\text{C}$  for 2 hours and 120  $^\circ\text{C}$  for 48 hours, were tested to evaluate the effects on BCS resistance and multipacting conditioning. The cavity was actively pumped during the baking procedure. The cavity vacuum was improved by 2 orders of magnitude during the 120  $^\circ\text{C}$  bake.

## CRYOGENIC TEST

### Cold Tests

The bare cavity was tested in between BCP steps and after hydrogen degassing. The cavity processing steps and cold test sequence are listed in Table 2. Each cold test was performed at both 4 K and 2 K in bath mode.

Table 2: Processing and Tests of Bare Prototype Cavity.

Test #	BCP	Integrated BCP	Heat treatment
1	60 $\mu\text{m}$	60 $\mu\text{m}$	N/A
2	80 $\mu\text{m}$	140 $\mu\text{m}$	N/A
3	60 $\mu\text{m}$	200 $\mu\text{m}$	50 $^\circ\text{C}$
4	20 $\mu\text{m}$	220 $\mu\text{m}$	600 $^\circ\text{C}$ + 120 $^\circ\text{C}$

### Q-E<sub>acc</sub> Curve

The Q-E<sub>acc</sub> curve of degassed and baked test (#4) is shown in Figure 5. The initial Q<sub>0</sub> is 3.1 $\times 10^9$  at 4 K and 1.9 $\times 10^{10}$  at 2 K. As the BCS resistance is negligible at 2 K for 325 MHz, the residual resistance is 4.9 n $\Omega$ . The ambient magnetic field in the cryostat is 35mG in the vertical direction. Assuming all magnetic flux is trapped in the superconducting transition, the calculated flux sensitivity [4, 5] of SSR1 is 0.12 n $\Omega$ /mG. The contribution of trapped flux to residual is estimated at 4.2 n $\Omega$ . Subtracting residual

component from 4K surface resistance results in a 4 K BCS resistance of 25.1 n $\Omega$ . The 2K Q curve has a more pronounced Q-slope in the medium field range compared to 4K curve. The slope is dominated by the field dependence of the residual resistance. Surface defects causing additional RF heating is suspected. The investigation is in progress. Cavity quenches limit cavity gradient at 10.3 MV/m at 2 K, corresponding to the nominal peak magnetic field of 63 mT, without detectable X-rays. The early quench could also suggest surface defects in the form of either geometry or foreign material.  $Q_0$  is  $4.0 \times 10^9$  at the nominal operational gradient of 9 MV/m, and the cavity power dissipation is 6.7 W.

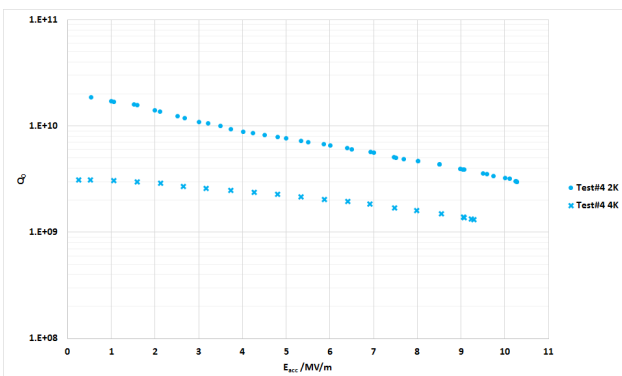


Figure 5: 4K and 2K  $Q$ - $E_{acc}$  curves of Test 4.

### Multipacting

The motivation of proposing the balloon variant is to reduce the likelihood of multipacting barriers near the operating gradient. This principle is proved through the cold tests. A comparison of measurement and simulation results is shown in Figure 6. The points in the figure represent cavity  $Q$  with multipacting loading. Both dotted line and dashed lines are the simulated growth rates of the secondary electrons. It indicates multipacting existing if the value is positive. The dashed line represents the first order barrier, while the dotted line represents the high order ones (order  $> 1$ ).

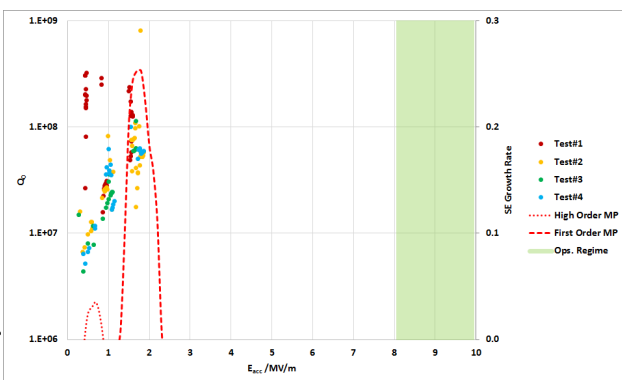


Figure 6: Comparison of measured and predicted multipacting barriers of SSR1.

Some conclusions are obtained as follows. There are no multipacting barriers either around the operational gradient or below 0.1 MV/m. The barriers only exist between 0.2

MV/m and 1.8 MV/m. The measurement results are consistent between tests and they are well predicted by 3D simulation codes, CST MWS and PS [6]. The simulated first order barrier is slightly over estimated in the higher gradient range (1.9 to 2.4 MV/m), while the simulated high order ones are under estimated (0.2 to 0.4 MV/m and 0.9 to 1.1 MV/m).

Multipacting conditionings were done at 4 K. Different manners were applied, such as pulse conditioning, amplitude modulation and frequency modulation. Pulse or step function drive provides a chance to jump over multipacting barriers and plunge into the higher gradient range. CW conditioning in self-excited loop was demonstrated as the best setting to clean up barriers. It is found that multipacting is unlikely to reappear after a completed conditioning.

The low temperature baking is verified to mitigate the intensity of multipacting. The baking procedures were performed at 50 °C for 2 hours and at 120 °C for 48 hours. Both recipes are effective to reduce the conditioning time by about 50 %. Removing the absorbed moisture and residual gas from the RF surface weakens the barriers. Consequently, bake at a lower temperature with a shorter period is more time-efficient for multipacting mitigation.

## CONCLUSION

The balloon variant of the single spoke resonator was proposed to mitigate multipacting around operational gradient. The first balloon cavity was designed, fabricated and tested by TRIUMF as the prototype of RISP SSR1. The bare cavity was processed with BCP, hydrogen degassing, HPR, and low temperature baking. The cold tests demonstrated the principle of the balloon concept. There is no multipacting barrier around the operational gradient. Several barriers exist in the low field regime, and are consistent with simulation. Low temperature baking also mitigates multipacting intensity. The  $Q$  curve shows good low field quality factor, but strong medium field  $Q$ -slope and early quench. Further investigation is in progress. The jacketed cavity test is underway and will be reported later.

## REFERENCES

- [1] H. J. Kim, H.C. Jung and W. K. Kim, "Progress on Superconducting Linac for the RAON Heavy Ion Accelerator," in *Proc. IPAC'16*, Busan, Korea, 2016, paper MOPOY039, pp. 935-937.
- [2] Z. Yao, R. E. Laxdal and V. Zvyagintsev, "Balloon Variant of Single Spoke Resonator," in *Proc. SRF'15*, Whistler, Canada, Sept. 2015, paper THPB021, pp. 1110-1114.
- [3] Z. Yao *et al.*, "Design and Fabrication of  $\beta=0.3$  SSR1 for RISP," in *Proc. LINAC'16*, East Lansing, MI, USA, 2016, paper MOPLR041, Sept. 2016, pp. 226-228.
- [4] D. Longuevergne and P. Duchesne, "Flux Trapping Studies on Low Beta Cavities at IPNO," INFN Milano University, Milan, Italy, Feb. 2018.
- [5] H. Padamsee *et al.*, *RF Superconductivity for Accelerators*. John Wiley & Sons, New York, 1998.
- [6] CST Studio Suite, <http://www.cst.com/>.